

OBSERVATIONS OF RED GIANTS WITH SUSPECTED MASSIVE COMPANIONS

VALERI V. MAKAROV

U.S. Naval Observatory, 3450 Massachusetts Ave., Washington, DC 20392-5420, USA

ANDREI TOKOVININ

Cerro Tololo Inter-American Observatory, Casilla 603, La Serena, Chile

Draft version February 11, 2019

ABSTRACT

Motivated by the existence of binary systems where a stellar-mass black hole is bound to a normal star, we selected four red giants with large radial velocity (RV) variation from the survey of SIM grid stars and monitored their RVs for several months. None turned out to contain a massive companion above 2.5 solar masses. The red giant TYC 9299-1080-1 with a large RV and a large proper motion is a single-lined spectroscopic binary with a period of 81 days. It is an extreme halo object moving at 350 km s^{-1} almost directly toward the Galactic center. HD 206092 is a double-lined binary with a short period of 4.37 days. It belongs to the rare class of active RS CVn-type binaries with evolved primary components, apparently undergoing mass transfer. The X-ray luminosity of HD 206092 is about twice as high as the most luminous coronal X-ray emitters observed by ROSAT, including II Peg and the prototype star RS CVn. HD 318347 has a variable double-peaked emission-line spectrum (not a giant), while HD 324668 has a constant RV. Despite the overall good quality of the SIM survey data confirmed by a comparison with Gaia DR2 mean radial velocities, the few large RV variations are explained, mostly, by erroneous data. We discuss the significance of the non-detection of massive companions in the SIM grid sample and the associated work.

Keywords: binaries — spectroscopic

1. INTRODUCTION

The first detection of gravitational wave signal, GW150914, by the LIGO and Virgo detectors incited a renewed interest in the evolution of binary systems including degenerate stars and black holes (Abbott et al. 2016). It showed that stellar-mass black holes (StMBH) with masses between $2.5M_{\odot}$ and several tens of solar mass should be present in binary systems in significant numbers, unless we were lucky to observe an exceedingly rare and fortuitous event. The detectable burst lasted for ~ 0.2 s, but it probably took billions of years for the binary system to go through the stages of evolution leading to this event, releasing approximately 3 solar masses of energy in the form of gravitational radiation. It is now up to observational astrophysics to confirm this scenario by finding StMBH in Galactic binaries.

Black holes in tight binaries with regular star companions are observable as powerful and variable X-ray sources. There are a few hundred known objects of this type in the Milky Way, but only two dozen have been dynamically confirmed as StMBH (Casares & Jonker 2014). The observable phenomena are caused not by the StMBH itself but by the high-energy processes in the accreted material. The orbital periods range from less than 3 hours to a month, but most are shorter than 1 day. Most of these tight X-ray binaries include a dwarf donor companion, but a few systems with giant companions are also known (Li 2015). The estimated masses of the BH companions are greater than $\sim 2.7 M_{\odot}$. Such tight systems must be the result of a long-term ($> 10^9$ yr) tidal

evolution or of rare dynamical events. However, it is reasonable to expect that the majority of Galactic StMBH reside in wider pairs with normal stars (separation < 1 AU for main sequence companions and a few AU for red giants), where there may be no or very little observable effects. There are three main possible ways to detect such binaries.

- Precision astrometry can reveal the reflex orbital motion of the stellar companion around the barycenter of the system. Based on the theoretical expectations of the rate of failed supernovae (e.g. Woosley & Weaver 1986), Gould & Salim (2002) predicted that ~ 30 binaries containing StMBH remnants are present in the Hipparcos catalog, but none has been found, owing to the limited sensitivity. Some candidate binaries have been reprocessed (Goldin & Makarov 2006, 2007), but the large uncertainty of the orbital parameters precluded definite detection of StMBHs. The renewed interest in this direction is focused now on the *Gaia* mission, which is expected to discover StMBH in scores (Mashian & Loeb 2017; Kinugawa & Yamaguchi 2018).
- Radial velocity (RV) variations can reveal large-amplitude orbital motion caused by a StMBH. Some systems in the 9th Catalogue (Pourbaix et al. 2004) have high values of the mass function, indicating a possible StMBH companion, but they are all of lower grades of reliability, with the exception of the well-studied X-ray binary HIP 18350 = X Per. More recent discoveries include candidates, such as the SB1 star AS 386, with $P = 131$ days,

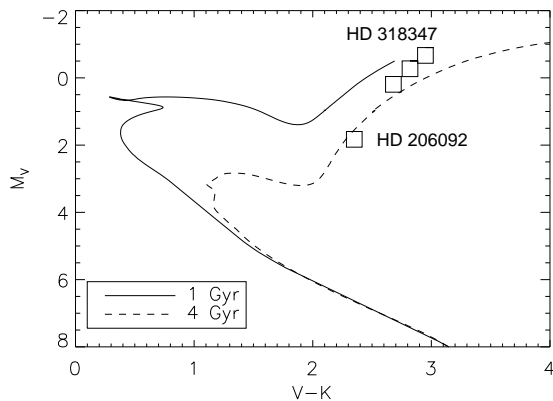


Figure 1. Location of the four candidates on the M_V , $V-K$ color-magnitude diagram. The lines are isochrones for solar metallicity and ages of 1 and 4 Gyr from Dotter et al. (2008). De-reddening corrections are not applied.

K_1 of 52 km s^{-1} , and mass function of $1.9 M_\odot$ (Khohlov et al. 2018).

- Precision photometry of eclipsing binaries reveals the presence of massive companions via the Eclipse Time Variation (ETV) effect. The *Kepler* main mission provided sufficient data for characterization of 222 triple systems (Borkovits et al. 2016). A few of those have high mass functions, suggesting a massive but invisible tertiary companion. However, the accuracy of this method is compromised by the large uncertainty of the period for long-term effects and the possible interference from persistent, differentially rotating photospheric spots.

In this work, we are exploiting the second method, i.e., the RV measurements of the reflex orbital motion. Our targets are selected from the extensive RV survey of southern sky red giants that had been suggested to serve as reference stars for the *Space Interferometry Mission* (SIM) (Makarov & Unwin 2015). The goal of this survey was to vet spectroscopically single stars, but a large fraction of binaries was discovered. Only 3 to 4 individual observations were typically made of each star in a campaign lasting 753 days; the sample size is 1134.

We selected from the above survey four stars with very large RV variation for further monitoring, with the aim to confirm their large amplitudes and determine the orbits. A large minimum mass of the secondary component derived from the spectroscopic orbit would provide a strong indication that the companion could be a StMBH and the object is a red giant (RG)+BH binary. The periods of such binaries are expected to be longer than ~ 100 days owing to the large radii of giants. Binaries with shorter orbital periods should go through the common envelope stage and end up as merged stars (prior to the core collapse) or as tight low-mass X-ray binaries (Ivanova et al. 2013). At periods longer than ~ 100 days, a giant star of $2 M_\odot$ orbited by a $5 M_\odot$ BH would have an RV amplitude of $K_1 = 60 \text{ km s}^{-1}$ if the orbit is seen edge-on. At longer periods P , the amplitude decreases as $P^{-1/3}$. A 2-year SIM grid survey could reveal RG+BH binaries with periods up to ~ 5 years.

None of our targets turned out to contain spectroscopically detectable massive companions. Nevertheless, the claimed large RV variation had to be verified and ex-

plained, revealing some intrinsically interesting and rare stars. The targets and our observing method are briefly introduced in Section 2. The following Section 3 presents our results regarding each star. The general discussion and conclusions are given in Section 4.

2. OBSERVATIONAL DATA

2.1. Targets

Four stars with large RV variations were selected from the SIM grid survey. Table 1 provides basic data on these stars: their common identifiers (they allow for the retrieval of other information from Simbad), visual magnitudes, spectral types, parallaxes, and short notes. Figure 1 shows the location of these stars on the $(M_V, V-K)$ color-magnitude diagram (CMD), computed using *Gaia* DR2 parallaxes (Gaia collaboration 2018) and the K magnitudes given by Simbad. No de-reddening corrections are applied. The stars are elevated above the main sequence, confirming the giant status.

2.2. CORALIE radial velocities

The RV survey of SIM grid stars was conducted by D. Queloz and D. Ségransan using the CORALIE echelle spectrometer at the 1.2-m Euler telescope in La Silla. The RVs were determined by cross-correlating the reduced spectra with the binary mask (Queloz et al. 2000). The cross-correlation function (CCF) contains a dip produced by all absorption lines included in the mask. Its position defines the RV, while the width of the dip depends on the width of the stellar lines (hence on the projected rotation velocity). The analysis by Makarov & Unwin (2015) shows the high overall quality of these RVs: the mean absolute error is 34 m s^{-1} , and the intrinsic RV jitter caused by the atmospheres of red giants is of the same order.

Observations reported here revealed that the large RV variability of our candidates was, mostly, caused by occasional erroneous measurements in the CORALIE data. As noted by D. Ségransan (2018, private communication), the CCF may not contain a valid dip for several reasons: very noisy spectrum (e.g. taken through the clouds), absence of absorption lines matching the mask, e.g. a star of early spectral type, or a large RV that falls outside the normally computed CCF window. In such cases, the processing software measures a wrong RV using the local CCF minimum. Outlying measurements could be identified and rejected by the low dip contrast. Problematic detections are further discussed in Section 3.

To confirm the overall high quality and variability of the SIM RV survey, we compared the data with the mean RVs from the Gaia Data Release 2 (DR2). We cross-matched 1133 stars in DR2, but only 1084 have RV measurements there. Selecting only stars with a probability of binarity (given in SIM RV) below 0.9, the resulting sample counts 697 stars. Fig. 2 shows the histogram of the RV unit weight error, i.e., the observed difference of $\text{RV}(\text{SIM})$ and $\text{RV}(\text{DR2})$ divided by the quadratic sum of their errors provided in both catalogs. The theoretically expected Normal[0, 1] PDF is shown for reference. In order to make the center of the empirical distribution coincide with 0, we added a common zero-point shift of 0.27 km s^{-1} to all individual differences. The presence of a systematic bias in DR2 measurements was discussed

Table 1
List of candidates

TYC	HD	V (mag)	Spectral type ^a	$\bar{\varpi}^b$ (mas)	Note
7381-433-1	318347	10.02	G0	0.729(0.052)	Emission star
7390-1610-1	324668	9.71	K0	1.009(0.042)	Constant RV
9299-1080-1	...	9.74	?	1.232(0.025)	SB1, 81 day
6948-350-1	206092	9.76	G9III	2.592(0.046)	SB2, 4.37 days

^a As given in Simbad

^b Parallaxes and errors are from the *Gaia* DR2 (Gaia collaboration 2018).

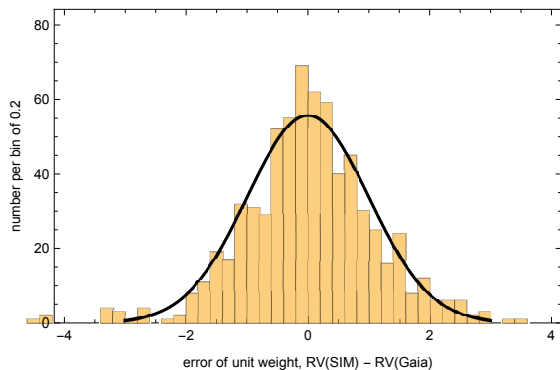


Figure 2. Histogram of normalized RV differences between the SIM RV survey and Gaia DR2 catalog for 697 common stars with binarity probability less than 0.9. The thick line shows the Normal[0,1] distribution for comparison. A common zero-point shift of $+0.27 \text{ km s}^{-1}$ was applied to all $\text{RV}(\text{SIM}) - \text{RV}(\text{Gaia})$ differences. The core of the empirical distribution is narrower than the expected distribution, indicating that the standard errors of mean RV may be slightly overestimated.

by Katz et al. (2018). Fig. 2 confirms that the bulk of RV measurements of constant stars are as precise as their standard errors suggest in both catalogs.

2.3. CHIRON observations

The observations reported here were conducted at the 1.5-m telescope located at Cerro Tololo (Chile) and operated by the SMARTS consortium. Ten hours of observing time were allocated through NOAO. Spectra were taken by the telescope operator in the service mode. The optical echelle spectrometer CHIRON (Tokovinin et al. 2013) was used in the fiber mode with a spectral resolution of 30000. On each visit, a single 5-minute exposure of the star was taken, accompanied by the spectrum of the comparison lamp for wavelength calibration. The data were reduced by the pipeline written in IDL.

The RVs are derived from the reduced spectra by cross-correlation with a binary mask based on the solar spectrum, similarly to the CORALIE RVs. We used 39 echelle orders in the spectral range from 4500\AA to 6500\AA , which is relatively less contaminated by telluric lines. More details are provided by Tokovinin (2016). The RVs delivered by this procedure should be on the absolute scale if the wavelength calibration is good. A comparison of CHIRON RVs with several RV standards revealed a small offset of $+0.16 \text{ km s}^{-1}$ (Tokovinin 2018b); in the following this offset is neglected. The mean RVs of the star with constant RV, HD 324668, measured by CORALIE and CHIRON, differ only by 43 m s^{-1} .

Table 2 gives the elements of two spectroscopic orbits derived from CHIRON RVs. The notations are standard, as is the method of orbit calculation by weighted least

squares. Individual RVs are given in Table 3, published in full electronically.

2.4. Speckle interferometry

All targets were observed on 2018.4 in the I band using the speckle camera at the 4.1-m SOAR telescope. The angular resolution (minimum detectable separation) was 50 mas, and the dynamic range (maximum magnitude difference) is about 4 mag at $0''.15$ separation. The instrument and observing technique are described in Tokovinin (2018a). No companions were detected.

3. NOTES ON INDIVIDUAL OBJECTS

3.1. HD 318347

Hydrogen emission in the spectrum of this star has been noted a long time ago. Simbad gives the spectral type G0, matching the red color $V - K = 2.96$ mag. However, the star is featured in the Catalog of galactic OB stars by Reed (2003).

The four CHIRON spectra taken over 165 days (from JD 2458260 to JD 2458425) do not have absorption lines typical of late-type stars, apart from the strong sodium absorptions, apparently of interstellar origin. The $\text{H}\alpha$ line shows a strong and wide emission with a double peak (Fig. 3). The strength of the emission and the contrast of the two peaks change on the time scale of a fortnight. The SIM grid catalog lists six RVs ranging from -245 to 323 km s^{-1} , all with small errors not exceeding 25 m s^{-1} . Suspiciously, two RVs measured with CORALIE on the same night, JD 2453591, differ by 54 km s^{-1} . These RVs were probably derived from the CCFs without valid dips, given the lack of absorption lines in the spectrum.

Most likely, HD 318347 is a highly reddened early-type star located in the Galactic plane at a distance of 1370 pc. However, Hou et al. (2016) find, based on LAMOST data, that most of the double-peaked $\text{H}\alpha$ emission line stars appear in binaries. A short-period cataclysmic variable cannot be precluded. It is possible that the unidentified *Fermi* Large Area Telescope (LAT) source 2FGL J1746.5 – 3228 (Nolan et al. 2012) is associated with the *Swift* X-ray source J174645.4 – 323746 (Paggi et al. 2013) and with HD 318347, which is located 5.8 arcsec away, a little more than the estimated positional uncertainty of the former. The 10\AA width of the $\text{H}\alpha$ emission implies gas motions at $\sim 500 \text{ km s}^{-1}$, possibly associated with accretion onto the stellar surface. Circumstellar material can cause additional extinction as well as the infrared excess.

3.2. HD 324668

This K0 giant is located in the Galactic plane at a distance of 1 kpc. The average of the three CHIRON RVs is

Table 2
Orbital elements

Name	P (day)	T_0 +2400000	e	ω (deg)	K_1 km s $^{-1}$	K_2 km s $^{-1}$	γ km s $^{-1}$	N	rms km s $^{-1}$
TYC 9299-1080-1	80.99 ± 0.02	58394.76 ± 0.08	0 fixed	0 fixed	18.41 ± 0.13	317.71 ± 0.08	13 ...	0.37 ...
HD 206092	4.37545 ± 0.00008	58271.347 ± 0.008	0 fixed	0 fixed	43.88 ± 0.87	111.69 ± 1.05	27.35 ± 0.50	17 ...	1.96 1.55

Table 3
Radial velocities

Name	JD -2400000	RV km s $^{-1}$	Comp.
HD 324668	58260.8470	-32.651	
HD 324668	58270.7916	-32.624	
HD 324668	58341.5915	-32.590	
HD 206092	58260.912	-6.810	a
HD 206092	58260.912	112.381	b
HD 206092	58271.899	59.516	a
HD 206092	58271.899	-50.498	b

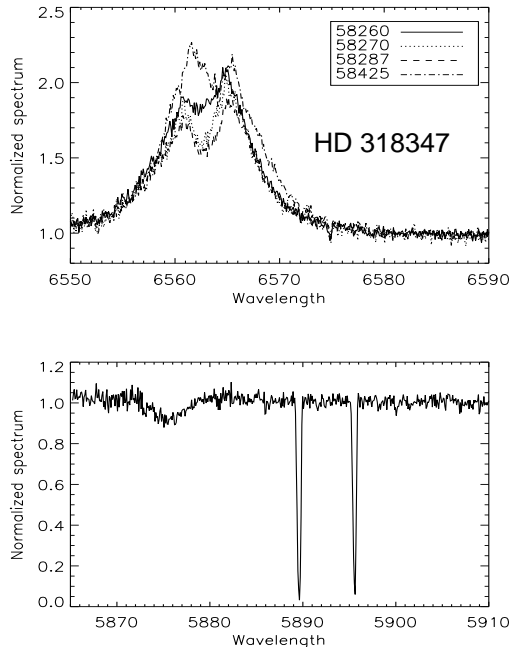


Figure 3. Two echelle orders in the spectra of HD 318347 containing the H α line (top) and the sodium D lines (bottom), normalized by the blaze function. Note the strong variability of the H α emission line strength in the spectra taken on four different MJD epochs.

-32.622 km s $^{-1}$ with an rms scatter of 31 m s $^{-1}$. They match perfectly the two RVs measured by CORALIE, with an average of -32.665 km s $^{-1}$. However, the third CORALIE RV of $+276.3$ km s $^{-1}$ is highly discrepant, earning this star a title of “Spectroscopic binary” in Simbad. We can only guess whether this discrepancy was caused by pointing at another star in this crowded sky region or for some other reason. Obviously, this red giant has a constant RV. Incidentally, it proves the excellent agreement between the RV zero points of CORALIE and CHIRON.

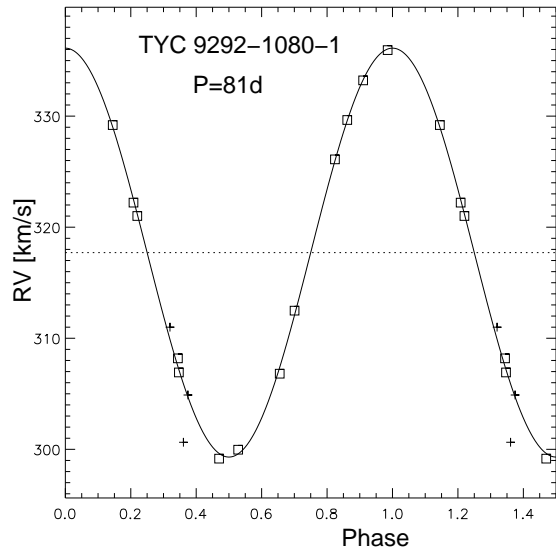
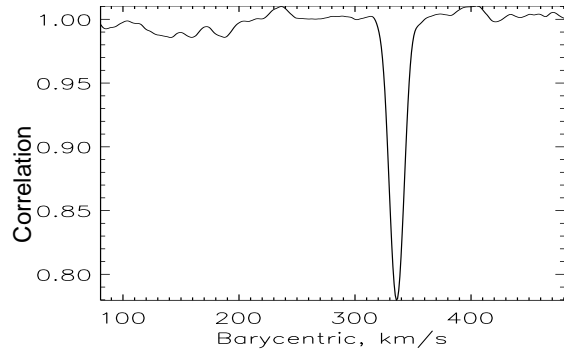


Figure 4. The CCF (top) and RV curve (bottom) of TYC 9299-1080-1. The crosses mark two RVs from CORALIE and one from *Gaia*.

3.3. TYC 9299-1080-1

This star, also known as CD-72 1472, is located at a distance of 812 pc and has a Galactic latitude of -25° . All three CORALIE RVs are mutually discordant: $+300.6$, -273.9 , and $+552.6$ km s $^{-1}$. They were measured over a time span of 696 days. The first CHIRON RVs have shown a slow trend, inspiring hope that this star has a long period and a large RV amplitude. However, further observations have shown that the RV varies with a period of 81 days. Elements of the circular single-lined orbit derived from 13 CHIRON RVs are presented in Table 2. The *Gaia* median RV of 311.0 km s $^{-1}$ roughly matches our orbit, assuming an epoch of 2015.5. The variability of the *Gaia* RV detections can be inferred from the elevated error of the median (5.7 km s $^{-1}$), which implies a single-measurement standard deviation of ~ 19 km s $^{-1}$. The first CORALIE RV fits

the orbit crudely. D. Ségransan (2018, private communication) provided another RV measured by CORALIE on JD 2454699.52, which matches the orbit perfectly. We attribute the two discrepant CORALIE RVs to the large RV of this star, placing the true dip outside the nominal CCF “window”. This explains why this object has two wrong RVs. However, the small errors of these erroneous measurements reported by the CORALIE pipeline, 22 and 16 m s^{-1} , are perplexing.

For the mass of the primary star in the range from 1 to 2 M_{\odot} , the minimum mass of the companion is from 0.48 to 0.73 M_{\odot} . The companion could be a normal solar-type dwarf or a white dwarf. The large radius of the giant primary has caused tidal orbit circularization. Its unusual feature is the large center-of-mass RV of 317.7 km s^{-1} . The parallax and proper motion correspond to the tangential velocity of 217 km s^{-1} , hence the star moves with a total velocity of 384 km s^{-1} relative to the Sun. Considering the Galactic rotation velocity at the solar radius, $236 \pm 3 \text{ km s}^{-1}$ (Kawata et al. 2019), and the solar peculiar velocity $(U_{\odot}, V_{\odot}, W_{\odot}) = (6.0, 10.6, 6.5) \text{ km s}^{-1}$ (Bobylev & Batkova 2014), we derive the galactocentric velocity of TYC 9299-1080-1, $(U, V, W)_{\text{gal}} = (302.9, 10.0, 66.2) \text{ km s}^{-1}$. This binary star certainly belongs to the Galactic halo. It moves almost straight toward the galactic center and will pass in its vicinity. However, the motion is not fast enough for a runaway or extragalactic star. Our numerical integration of the Galactic orbit indicates that it moves on a highly extended orbit between $\sim 100 \text{ pc}$ and 20 kpc from the center, which will be reached in less than 20 Myr.

3.4. HD 206092

Located at a distance of 386 pc, this object is the closest of our four candidates. Its association with a ROSAT X-ray source was noted, while Kiraga (2012) found photometric variability with a period of 2.1876 days, presumably caused by rotational modulation.

The first CHIRON spectra revealed wide double lines in rapid motion (Fig. 5). The system’s location in the CMD (Fig. 1) indicates that the primary is an evolved star, probably a red giant. Thus, this system belongs to the rare type of RS CVn-type binaries characterized by high levels of chromospheric and X-ray activity. Further monitoring established the orbital period of 4.38 days. The orbit (Table 2) is circular, with amplitudes of 44 and 112 km s^{-1} . The residuals of CHIRON RVs to the orbit are relatively large because the CCF dips are wide and have somewhat irregular shapes, presumably caused by starspots. The photometric period found by Kiraga (2012) corresponds to half of the orbital cycle, indicating ellipsoidal variability caused by tidally distorted stars in a close binary. The Balmer lines $H\alpha$ and $H\beta$ in the spectra of HD 206092 are shallow, being filled by emission; the sodium D lines also have emission in their cores produced in the chromosphere.

In this case, the large RV variability detected by CORALIE is explained by the orbital motion. We compared these six RVs with our orbit and found that one is highly discrepant, three correspond to the primary component Aa and two match the secondary Ab. These RVs were used with low weights to improve the accuracy of the period. The RV errors reported by CORALIE for

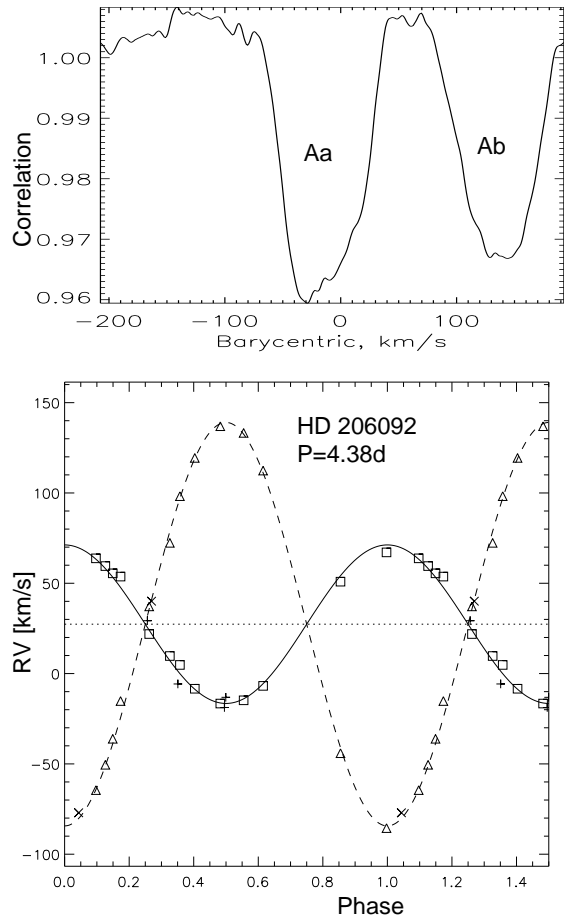


Figure 5. The CCF on JD 2458356 (top) and the RV curve (bottom) of HD 206092. Squares and full line denote the primary component Aa, triangles and dashed line correspond to the secondary Ab. Crosses and plus signs depict the CORALIE RVs.

this star are unrealistically small.

The orbit corresponds to the minimum masses $M_1 \sin^3 i$ and $M_2 \sin^3 i$ of 1.22 and 0.48 M_{\odot} , or the mass ratio of 0.39. Yet, the areas of the CCF dips are comparable, indicating the light ratio of 0.82 (see Fig. 5). Assuming the mass sum of 2 M_{\odot} , the orbital axis is 14.2 R_{\odot} . The wide CCFs suggest that the components almost touch each other; the large luminosity and the red color correspond to large stellar radii. The roughly estimated $v \sin i$ (projected surface velocity of rotation) is 40 km s^{-1} , hence, the radii for both components $R > 3.5 R_{\odot}$ assuming synchronous rotation. The unusually bright (for its mass ratio) secondary component Ab must be transferring mass to the primary component Aa. We tried to find analogues of HD 206092 by selecting binaries with the following parameters: period < 10 days, $V - K > 2$ mag and $M_V < 2.5$ mag. The only analogue we found is RS CVn (HD 114519), the prototype of its class, which is defined as chromospherically active, short-period binaries with primaries evolved off the main sequence (Fekel et al. 1986). The corresponding parameters for RS CVn are $P = 4.80$ days, $M_V = 2.5$ mag, $V - K = 2.16$ mag, spectral type K0IV. Not surprisingly, the object is a powerful source of coronal X-ray emission listed in the ROSAT catalog of bright sources.

Looking at evolved binary systems with somewhat longer periods, the large mass ratio and similar line

strengths of HD 206092 suggest that it is similar to chromospherically active semi-detached eclipsing binaries such as AR Mon and RZ Cnc (Popper 1976). Although AR Mon and RZ Cnc have significantly longer periods (20 days) than HD 206092, they appear to be in a similar mass transfer evolutionary stage. Another similar large mass ratio system, which has a shorter period of 10.7 days, is RV Lib (Imbert 2002).

Using a ROSAT-determined count rate $CR = 0.176(0.023)$ cts s^{-1} and a hardness ratio of $HR1 = 0.44(0.13)$ we derive an X-ray luminosity of $L_X = 3.34(0.066) \times 10^{31}$ erg s^{-1} , where the standard error is estimated from the formal uncertainties of the CR, HR1, and Gaia parallax. RS CVn-type binaries are the most luminous (and, on average, the hardest) sources of coronal X-ray radiation (Makarov 2003), but HD 206092 is almost twice as luminous as the brightest X-ray star within 50 pc of the Sun, which is II Peg, also a RS CVn-type binary. Another useful comparison is the prototype star RS CVn (F6IV+G8IV) with $L_X = 1.67(0.01) \times 10^{31}$ erg s^{-1} . This puts HD 206092 into the category of outstandingly active and X-ray luminous field stars.

4. DISCUSSION AND CONCLUSIONS

4.1. Expected number of RG+BH binaries

In the past, considerable effort has been spent to predict the number of binaries containing compact objects, focusing mostly on potential sources of gravitational waves generated by merging binaries with two compact components (e.g. Belczynski et al. 2002). These works use binary population synthesis. The results depend strongly on the initial assumptions such as binary statistics and are also affected by the uncertainties in the binary and stellar evolution. The same population-synthesis approach was used more recently to estimate the number of star-BH binaries detectable by *Gaia* through astrometric effects of unseen companion on the visible star. Predictions made by different groups differ by two orders of magnitude, depending on the assumptions and models used (Kinugawa & Yamaguchi 2018).

All massive binaries with orbital separations less than 20 AU are affected by the mass transfer and mass loss that changes their orbits (Moe & Di Stefano 2017). Large velocities acquired by the remnants during supernova explosions (“kicks”), on the order of hundreds of km s^{-1} , likely destroy all binaries except the tightest ones. Hence, it is possible that RG+BH binaries with periods longer than ~ 100 days do not exist¹.

Neglecting both orbital evolution and kicks, we estimate the fraction of RG+BH progenitors, i.e. the upper limit of the fraction of RG+BH binaries among red giants. The progenitors of BH components have masses $M_0 > 20M_\odot$ (Belczynski et al. 2002), while the giants have typical masses between $M_1 = 2M_\odot$ and $M_2 = 3M_\odot$.

¹ Several *low mass* X-ray binaries with giant components have been identified, however. For example, symbiotic X-ray binaries are a rare class of low-mass, hard X-ray binaries that consist of a neutron star accreting mass from an M giant. Two systems so far have been analyzed, V2116 Oph (Hinkle et al. 2006) and V934 Her (Hinkle et al. 2018) and both have long periods, of 3.2 and 12.0 years, respectively. Thus, at least for supernova remnant binaries that result in neutron stars, some long-period systems do survive.

Using the Salpeter mass function $f(M) \propto M^{-\alpha}$ with $\alpha = 2.35$, we evaluate the fraction of stars more massive than M_0 relative to stars with masses between M_1 and M_2 , $f_* = 0.106$. Now, some fraction of stars with $M_0 > 20M_\odot$ are binaries with secondary components in the same mass range as our giants, between M_1 and M_2 , and with periods from 100 to 10^3 days. These binaries are potential progenitors of RG+BH objects when their primary components become black holes and the secondaries turn into giants. The fraction of such progenitors relative to field stars in the same mass range (which also become giants) can be estimated using the recent analysis of binary statistics by Moe & Di Stefano (2017). About $f_B = 0.2$ of massive stars have binary companions of all masses in the above period range. At those periods, the distribution of the mass ratio q does not follow the Salpeter function, although it still grows as $q^{-1.5}$ at $q > 0.3$. Therefore, the fraction of massive stars with suitable parameters is $f_B f_q$, where $f_q \approx 0.2$ is the fraction of companions in the selected mass range between M_1 and M_2 . Summarizing, for each primary star in this mass range we get $f_* f_B f_q = 0.004$ potential progenitor binaries.

A sample of 1000 giants is not expected to contain more than 4 progenitors of RG+BH binaries with intermediate periods. Given the evolution of binary orbits and the destructive effects of the supernova kicks, the expected number of RG+BH binaries should be much less than the number of their progenitors. Hence, the non-detection of such objects in the SIM grid survey is natural.

4.2. Related work

Recently, Murphy et al. (2018) introduced a new observing technique by deriving “spectroscopic” orbits from the timing of stellar pulsations. They presented a sample of 314 such orbits for primary stars of A/F spectral types and periods between 100 and 1500 days, progenitors of the red giants studied here. The size of the parent sample was 2224, twice as big as the SIM grid sample. They estimated that a fifth of these binaries have degenerate white-dwarf secondaries, while their primaries are products of mass transfer (blue stragglers). None of the binaries had a large mass function indicative of the BH secondary. This non-detection of BH secondaries agrees with our result.

Using population synthesis, Kinugawa & Yamaguchi (2018) estimated the number of binaries with BH components detectable astrometrically by *Gaia*. Their assumptions regarding binary statistics differ from the latest analysis by Moe & Di Stefano (2017) in several important respects. The predicted fraction of BH binaries with periods between 50 days and 5 years (similar to the period range explored here) in a simulated sample of 10^5 progenitor binaries ranges from 0.013 to 0.028, depending on the metallicity (more BH binaries in metal-poor population). The majority of these binaries contain stars less massive than $2 M_\odot$. We stress that these estimates are highly uncertain.

4.3. Conclusions

The large RV variability of some red giants detected by the CORALIE survey of SIM grid stars was intriguing and called for further investigation. We found that

this detection is spurious, resulting from flukes in data reductions.

Theoretical estimates, still highly uncertain, indicate that the fraction of red giants containing a StMBH remnant cannot exceed 10^{-2} , and likely is orders of magnitude smaller. Yet, observational limits on the existence of such RG+BH binaries should be placed independently of the theory. Our study contributes to establishing such limits by non-detection of RG+BH candidates in a sample of 1000 stars.

Among the four candidates studied here, two can be of independent interest: the red-giant binary TYC 9299-1080-1 with a large spatial velocity of 384 km s^{-1} and the semi-detached binary HD 206092 of the rare RS CVn type.

ACKNOWLEDGMENTS

We thank the telescope operator R. Hinohosa for taking the data. D. Ségransan has kindly helped us to understand the origin of discrepant CORALIE RVs and provided additional unpublished RV of TYC 9299-1080-1.

REFERENCES

- Abbott, B. P., et al. 2016, *Phys. Rev. Lett.* 116, 24
 Belczynski, K., Kalogera, V., & Bulik, T. 2002, *ApJ*, 662, 504
 Bobylev, V. V. & Batkova, A. T., 2014, *MNRAS* 441, 142
 Borkovits, T., Hajdu, T., Sztakovics, J., et al. 2016, *MNRAS*, 455, 4136
 Casares, J., & Jonker, P. G. 2014, *Spa. Sci. Rev.*, 183, 223
 Dotter, A., Chaboyer, B., Jevremović, D., et al. 2008, *ApJS*, 178, 89
 Fekel, F. C., Moffet, T. J., & Henry, G. W. 1986, *ApJS*, 60, 551
 Gaia Collaboration, Brown, A. G. A., Vallenari, A., Prusti, T., et al. 2018, *A&A*, 595A, 2 (Vizier Catalog I/345/gaia2).
 Goldin, A. & Makarov, V. V. 2006, *ApJS*, 166, 341
 Goldin, A. & Makarov, V. V. 2007, *ApJS*, 173, 137
 Gould, A. & Salim, S. 2002, *ApJ*, 572, 944
 Hinkle, K.H., Fekel, F.C., Joyce, R.R., et al., 2006, *ApJ*, 641, 479
 Hinkle, K.H., Fekel, F.C., Joyce, R.R., et al., 2018, arXiv:1812.08811
 Hou, W., Lou, A.-Li, Hu, J.-Y., et al. 2016, *RAA*, 16, 138
 Imbert, M. 2002, *A&A*, 387, 850
 Ivanova, N., Justham, S., Chen, X., et al. 2013, *A&ARv*, 21, 59
 Katz, D., Sartoretti, P., Cropper, M., et al. 2018, arXiv:1804.09372
 Kawata, D., Bovy, J., Matsunaga, N., & Baba, J. 2019, *MNRAS*, 482, 40
 Khokhlov, S. A., Miroshnichenko, A. S., Zharikov, S. V., et al. 2018, *ApJ*, 856, 2
 Kiraga M., 2012, *Acta Astron.*, 62, 67
 Kinugawa, T. & Yamaguchi, Y. S. 2018, arXiv:1810.0972
 Li, X.-D. 2015, *New Astronomy Reviews*, 64, 1
 Makarov, V. V. 2003, *AJ*, 126, 1996
 Makarov, V. V. & Unwin, S. C. 2015, *MNRAS*, 446, 2055
 Mashian, N., Loeb, A. 2017, *MNRAS*, 470, 2611
 Moe, M. & Di Stefano, R. 2017, *ApJS*, 230, 15
 Murphy, S. J., Moe, M., Kurtz, D. W., et al. 2018, *MNRAS*, 474, 4322
 Nolan, P.L., Abdo, A.A., Ackermann, M., et al. 2012, *ApJS*, 199, 31
 Popper, D.M. 1976, *ApJ*, 208, 142
 Pourbaix, D., et al. 2004, *A&A*, 424, 727
 Queloz, D. et al. 2000, *A&A*, 354, 99
 Paggi, A., Massaro, F., Abrusco, R.D., et al. 2013, *ApJS*, 209, 9
 Reed, B. C. 2003, *AJ*, 125, 2531
 Tokovinin, A., Fischer, D.A., Bonati, M., et al. 2013, *PASP*, 125, 1336
 Tokovinin, A. 2016, *AJ*, 152, 11
 Tokovinin, A. 2018a, *PASP*, 130, 5002
 Tokovinin, A. 2018b, *AJ*, 156, 48
 Woosley, S. E. & Weaver, T. A. 1986 *ARA&A*, 24, 205